Characterization of undocumented CO_2 hydrothermal vents in the Mediterranean Sea: implications for ocean acidification studies

Michela D'Alessandro[1]* , Maria Cristina Gambi[1]* , Cinzia Caruso[2], Marcella Di Bella[2,3], Valentina Esposito[1,4], Alessandro Gattuso[2], Salvatore Giacobbe[5], Martina Kralj[1], Francesco Italiano[2], Gianluca Lazzaro[2], Giuseppe Sabatino[5], Lidia Urbini[1], Cinzia De Vittor[1]

[1] National Institute of Oceanography and Applied Geophysics – OGS, Trieste (Italy)
[2] Istituto Nazionale di Geofisica e Vulcanologia – INGV, Palermo e Sede operativa di Milazzo (Italy)
[3] Sede Territoriale Sicilia, Department of Integrated Marine Ecology, Stazione Zoologica Anton Dohrn (SZN), Milazzo (Italy)
[4] Stazione Zoologica Anton Dohrn, Research Infrastructures for Marine Biological Resources Department, Via Po 25, 00198 Roma (Italy)
[5] Department of Chemical, Biological, Pharmaceutical and Environmental Sciences, ChiBioFarAm, University of Messina (Italy)
[6] Department of Mathematical and Computer Sciences, Physical Sciences and Earth Sciences, University of Messina (Italy)
*corresponding authors
E-mail: mdalessandro@ogs.it
gambimc@gmail.com

Abstract

In this paper, we present the first multidisciplinary description of an undocumented hydrothermal field located in Sicily (Southern Tyrrhenian Sea), at water depths ranging from 0 to 5 m. The area and the associated living communities were visually explored (snorkeling and SCUBA diving) in June 2021. Twenty sites were investigated for pH, alkalinity and nutrients analysis. Geochemical investigation of hydrothermal fluids gases revealed CO_2 dominance (98.1%) together with low amount of oxygen and reactive gases. Helium isotope ratios (R/Ra =2.51) and $\delta^{13}C_{CO2}$ (3) seem to confirm an inorganic origin of hydrothermal degassing of CO_2 and the ascent of heat and deep-seated magmatic fluids to the surface. Values of pH ranged between 7.84 and 8.04, ΩCa between 3.68 and 5.24 and ΩAr from 2.41 to 3.44. Visual census of fish and megabenthos revealed the presence of 62 species among which five protected by SPA/BIO Protocol and two by the International Union for Conservation of Nature. This study represents the first step for the description of a suitable area of considerable interest for future ocean acidification experimental studies.

Introduction

Hydrothermal vents are worldwide recognized for their biological, ecological, cultural and economic importance [1, 2]. These areas are characterized by rising of gases and fluids, which make them highly productive areas able to supply important benefits to humans and ecosystems [3]. Among ecosystem services provided by vents, there are provision, regulation and cultural ones. The first ones are related to the high rates of chemosynthetic production due to microorganisms that transform inorganic elements coming out from the seafloor, such as H_2S, CH_4, Fe^{2+}, to produce

energy [4]. This high primary production generates enrichment of secondary production and fishery resources, with subsequent economic benefits to humans [3]. Among the welfares by hydrothermal vents, there is also the supply of metabolites and bioactive molecules produced by some organisms to survive in these extreme conditions, and used by cosmetic and pharmaceutic industries [5].

The regulation services supplied by hydrothermal vents regard the biogeochemical cycle of elements and their effects on climate and carbon sequestration. Indeed, the uptake of sulphide and methane by bacterial decreases the emission of these substances in the atmosphere [6].

In terms of cultural services, the hydrothermal ecosystems represent interesting study areas in the different fields of science from biology to studies on the origin of life in the universe and on global change [7, 8].

Hydrothermal fields are reported within a wide range of depths from intertidal to abyss and are characterized by different living communities [9, 10]. Generally, the deep hydrothermal vents (> 200 m) are inhabited by a typical fauna characterized by obligate taxa and symbiotic species as siboglinid tubeworms, large bivalves and snails [9]. Many new or rare species in deep vents have been described in association with these systems [10].

On the contrary, shallow-water hydrothermal vent (< 200 m) are more limited than deep ones [9], and their communities are not different from the neighbour ones [10], although recently also in shallow-waters vents a few new and rare species have been observed [11, 12], which may lead to consider these systems as evolutionary laboratories, as the deep habitat. In addition, shallow-water vents are of particular interest since they often can be reached by direct exploration (SCUBA diving) and more suitable for experimental and manipulative research [13].

The bubbling of fluids, especially CO_2 and other gasses from the seafloor, acidify the surrounding vents' environment making them an ecological analogue of what is expected in the scenario of the future ocean as a consequence of Ocean Acidification (OA) [13, 14, 15].

For this reason, hydrothermal ecosystems are increasingly used as natural laboratories to analyse biological and physiological responses at species and community levels to OA [16, 17]. In addition, the lowering of pH, typical of these areas, generates a complex set of environmental features, such as oxygen reduction, alteration of nutrients and of species interaction that are usually difficult to reproduce in mesocosms [18, 19].

The biological peculiarities distinguishing deep and shallow hydrothermal areas are mainly tied to differences in their chemical complexity. In fact, shallow-water hydrothermal systems are characterized by lower pressure and fluids that may be derived from meteoric water, seawater and magmatic fluid in variable amounts. The groundwater flow can be influenced by different sources, such as the hydraulic gradient, rock type, and tidal pumping [20]. On the contrary, the deep-sea hydrothermal fluids are derived exclusively from seawater except in special cases where magmatic fluids are involved [21, 22].

Shallow-water vents ecosystems are relatively rare. Nowadays, about 25 shallow hydrothermal vent's systems are studied around the world as proxy to study the effects of climate change and OA [13, 15, 23, 24] receiving further impulse by recent developments of exploration and detection methods [25]. A few other systems have been described recently [15, 26, 27]. There is a relatively large body of research on the species and communities inhabiting shallow hydrothermal vents characterized by OA conditions, and also a few reviews on the main structural changes showing a general reduction of taxonomic and functional diversity in the areas of major venting and critical low pH conditions [13, 16, 24].

In the Mediterranean Sea, hydrothermal areas are reported in the Tyrrhenian, Balearic and Aegean Sea. In the Tyrrhenian, the areas characterized by hydrothermalism are in the Aeolian archipelago, at Vulcano, Stromboli, Filicudi and Panarea Islands and nearby islets, at Capo Palinuro (Campania), at the Pontine Archipelago (Latium), and at Ischia island and the Bay of Naples [28, 29, 30]. In the Balearic Sea, a vent systems has been described at the Columbretes islands [31], while in the Aegean, major hydrothermal vent systems are found along the Volcanic Arc at Euboea, Milos, Santorini, Kos, and Yali Nisiros [27, 32].

The aim of this paper is to provide the first multidisciplinary description of a new discovered CO_2-rich hydrothermal site located in the southern Tyrrhenian Sea, with the objective to characterize the area and discuss the implications of its use in ocean acidification experimental studies.

Geological setting of the investigated hydrothermal area

The studied hydrothermal area is located in the Gulf of Patti (San Giorgio di Gioiosa Marea locality), NE Tyrrhenian coast of Sicily (Figure 1 and 2).

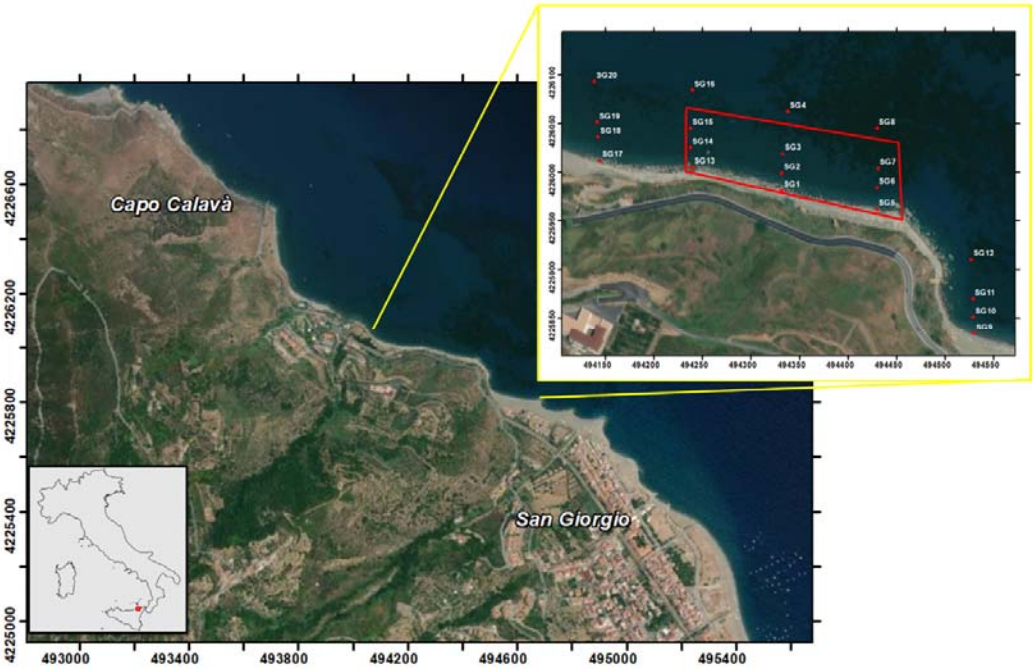

Figure 1: The study site and sampling spots. The hydrothermal field of San Giorgio is highlighted by the red polygon. Map made by means of ArcMap 10.5, ESRI software.

The area belongs to the regional tectonic structure known as Aeolian-Tindari-Letojanni NW-SE faults system (ATLFS), which extends from the central sector of the Aeolian Islands (Salina, Lipari and Vulcano) to the Ionian Sea [33, 34, 35]. It represents one of the most seismically active regions of the Italian Peninsula [34, 35] and is linked to the general geodynamic scenario of the central Mediterranean dominated by convergence between the European and African plates [36, 37, 38].

Recently, CO_2 degassing along the southernmost portion of the ATLFS (Nebrodi-Peloritani Mountains), onshore from the investigated area, has been revealed by Italiano et al. [30] that suggested a crustal and/or mantle source for the involved fluid emissions. Moreover, in the nearby Aeolian volcanic archipelago, offshore from the investigated area, intense submarine volcanic processes and degassing activity, mainly visible at Vulcano and Panarea islands have been widely reported and studied [39]. CO_2 vents of Panarea represent the large hydrothermal systems of the

whole Mediterranean sea, in which in early November 2002 occurred a submarine gas burst near the Bottaro islet, which generated a submerged crater [40].

Figure 2: Image of one of the high intensity gas emissions form the bottoms of the San Giorgio hydrothermal vents

Results

Abiotic investigation

Water analyses

All the dissolved inorganic nutrients showed the highest values in TR5, out of the direct bubbling of the vents on the westwards side. Ammonia ranged between non detectable (<0.01 µmol L^{-1}) to 0.05 µmol L^{-1} (stations SG17 and SG18) (Figure 3, Supplement Table S1).

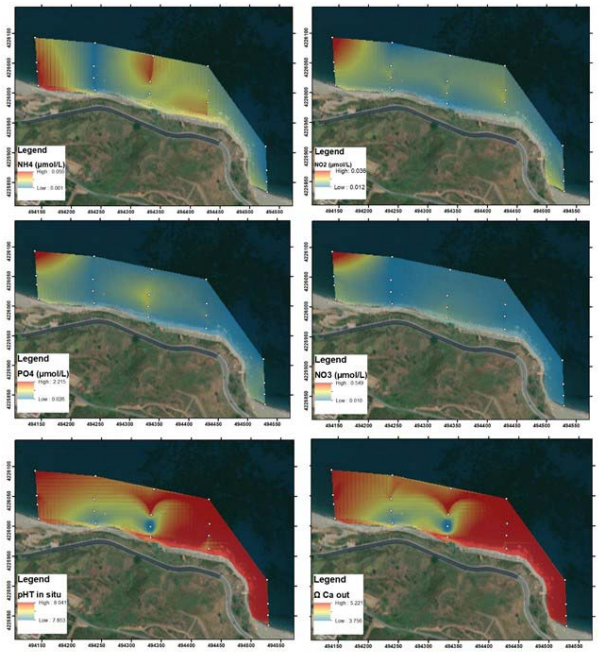

Figure 3: Natural Neighbour spatial interpolations of the main representative abiotic parameters recorded in the San Giorgio vents study area. Map made by means of ArcMap 10.5, ESRI software.

$Si(OH)_4$ ranged between 0.78 µmol L^{-1} in SG15 to 1.36 µmol L^{-1} in SG17. In addition, NO_3 and PO_4 shows the highest value in SG17 (0.14 µmol L^{-1} and 2.24 µmol L^{-1}, respectively), while NO_2 showed the highest value in SG20 (0.04 µmol L^{-1}). AT ranged between 2521.47 µmol kg^{-1} (SG3) to 2533.5 µmol kg^{-1} (SG4). The lowest ΩCa out and ΩAr out were both recorded in SG2, with a value of 3.68 and 2.41, respectively.

Gas Analyses

The gas analysis revealed CO_2 as the dominant gas component (98.1%), followed by N_2 (1.02%), CH_4 (0.43%), H_2S (0.35%); O_2 (0.14%). In addition, very low percentage were also found for He, H_2 and CO (0.0015, 0.0007 and 0.0005%, respectively). Helium isotope ratios display values in the range of 2.51 Ra (Table 1).

R/Ra	He/Ne	$\delta^{13}C_{CO2}$	He %	H_2 %	O_2 %	N_2 %	CO %	CH_4 %	CO_2 %	H_2S %
2.51	177.22	3	0.0015	0.000698	0.14	1.02	0.0005	0.43	98.1	0.35

Table 1. Chemical and isotopic compositions of the sampled gas emissions. All the chemical concentrations are expressed in mol%. The helium isotopic composition is expressed as R/Ra, where R is the 3He/4He ratio in the sample and Ra is the same ratio in the atmosphere. The carbon isotopic composition is given versus PDB.

The most abundant percentage of CO_2 recorded at the air-water interface was of 1.73 % (Table 2).

	North (m)	East (m)	CO_2 %
# 1	4226017	494330	0.7
# 2	4226016	494331	1.17
# 3	4226019	494332	0.85
# 4	4226024	494335	0.35

Table 2. Percentage of CO_2 recorded on four samples of air-water layer collected on the SG2 station. Coordinate are expressed in UTM WGS84, Zone 33 S .

	Output (litres/min)	Point emissions	Measured emissions	Total output (litres/ min)	Typology of emissions
Flux 1	1	14	1	14	High
Flux 2	1.2	5	1	6	High
Flux 3	0.25	15	1	3.75	Medium
Flux 4	0.1	40	1	4	Low
Flux 5	0.1	30	1	3	Low

Table 3. Total output of gases and typologies of emission flux recorded on five different sites.

A total flux of gasses of 30.75 litres/minutes has been estimated to be emitted in the whole area of the San Giorgio hydrothermal vents (Table 3).

Environmental description and biotic investigation

The seafloor along all transects examined parallel to the coastline is composed by a mosaic of coarse sediments (mainly coarse sands) interspersed with stones (>1 m), rocks/boulders (<1 m) and patches of *Posidonia oceanica*. On the sandy bottom, where intense venting is present, sub-circular

rusty patches, probably due to the precipitation of metal oxides, occur. The areas close to the emissions in correspondence of rocks or large boulders are often colonized by microbial white mats. A total of 62 taxa: 9 macrophytes, 29 invertebrates and 24 fishes have been censuses (see list in Supplement Table S2).

Among the algae, all the species found were typical of the shallow photophilous hard bottoms as *Padina pavonica, Halopteris scoparia, Anadyomene stellata, Ellisolandia elongata, Jania rubens* and *Codium bursa*. Among the invertebrates most of the species were molluscs (25%), mainly gastropods associated with vegetated hard bottoms, but also the two bivalves *Chamelea gallina* and *Donax trunculus* that are associated with soft sediments (sands), and the bivalve *Pinna rudis* associated with Posidonia meadows. At the edge of the vent's field, in fact, a vast meadow of the seagrass *Posidonia oceanica* extends. Two alien species were recorded, the green alga *Caulerpa cylindracea* and the crab *Percnon gibbesi*. The ichthyofauna was characterized by several species as *Coris julis, Chromis chromis, Diplodus annularis, Mullus barbatus, Thalassoma pavo, Trachinotus ovatus* and juveniles of two species of *Epinephelus*, i.e. *E. costae* and *E. marginatus*, considered as vulnerable and endangered in the IUNC list. Juveniles stages of various other bony fishes were recorded, such as *C. chromis, Diplodus vulgaris, M. barbatus, T. ovatus, T. pavo, Symphodus tinca* and *Sparisoma cretense*.

Here we shortly describe each transect to characterize the main bottom features and the most frequent benthic and fish species.

At transect 1 (approx. 1 m depth, 109 plots analysed) the bottom is characterised by stones and sand, that are recorded with about the same frequency percentage of plots (82.6 and 81.7%, respectively). Boulders/rock were recorded in 22% of plots, and very few tufts of *P. oceanica* only in the 2.7% of plots. Both boulders/rock and stone were colonized for 92.7% by benthic organisms mainly represented by turf and erected algae. The species recorded with the highest frequency was *Halopteris scoparia* (47.7% of the plots), followed by *Jania rubens* (28.4%) and by the sponge *Sarcotragus foetidus* (14.7%). Several species were recorded with frequencies less of 10%: the coralline algae *Ellisolandia elongata* (7.3%), the sponges *Ircinia irregularis* (5.5%) and *Crambe crambe*, the green alga *Anadyomene stellata* and the cnidarian *Pennaria disticha* (both with 2.8%). On the rocks and stones, the gastropod *Patella caerulea* (1.8%), *Stramonita haemastoma* (0.9%) and *Cerithium vulgatum* (0.9%) were also observed. Gas emissions of different intensities appeared in 30 plots; 5 scattered and 7 continuous plots. Along the transect, 12 bony fish species were observed: *S. tinca* (17.4%), followed by *C. chromis* (12%), *D. vulgaris* (10%). The lower frequencies were recorded for *E. costae* and *E. marginatus* (both with 0.9%).

At transect 2 (approx. 2 m depth, 96 plots analysed) the bottom is composed by a mosaic of various substrate types: stones, occurring in 92.6% of the plots and covering a mean of 54% of the bottoms, followed by boulders/rock with 57% frequency and 50% bottom covered, sands, although present in 82% of the examined plots, covered only a mean of 10% of the sea bottom. Stones showed an average colonization by benthic organisms of 55%, while boulders/rock showed a mean colonization of 65%. *Posidonia oceanica* was present with very small patches in 22% of the plots and with a modest mean cover of 12%. Finally, gas emissions of different intensity were encountered in 13 and 4 contiguous plots. The stones and rock are mainly colonized by a turf of small filamentous algae (97% of the plots), followed by other 4 species of macroalgae such as *Padina pavonica* (78.1%), *J. rubens* (58.3%), *H. scopari*a (32.6%) and *A. stellata* (7.3%); while among the invertebrate only the sponge *Sarcotragus foetidus* was dominant, occurring in 73% of

the plots. Other species recorded with modest frequency were *Vermetus triquetrus* (3%), and *Hexaplex trunculus* (4%). Seven taxa of bony fishes were observed, all with low frequencies: *C. chromis* (6.3%), *S. salpa* (4.2 %), *D. vulgaris* (3.1%), *O. melanura*, *S. cabrilla*, *T. pavo*, *Triperigion* sp. (all with 2.1%).

At transect 3 (approx. 2.5-3 m depth; 85 plots examined) the bottom shows still a mosaic of different substrate types, with an increase of boulders/stones (64% of the plots) and higher mean bottom cover (59%), and also a higher frequency of Posidonia patches, occurring in 62% of the plots and with a mean cover of 23.4%. Sand patches are still frequent (63%) although with modest mean cover (17%), as well as stones (45% frequency and 24% cover). Gas emissions were encountered in 3 scattered and 4 contiguous plots. At this depth, both stones and rocks show much higher level of benthic colonization with respect to transect 2, with a mean of 66.8% for stones and 85% for boulders/rocks. The hard substrates are still colonized mainly by turf algae (95.5%) and by the previous four macroalgae, which increased their frequencies, *J. rubens* (72.9%), *P. pavonica* (89.4%), *H. scoparia* (71%), *A. stellata* (7.1%), and among the invertebrates still the most conspicuous species is *S. foetidus* (77.7%), followed by *V. triquetrus* (6%), the sponge *Crambe crambe* (3.4%) and colonial hydroids (likely *Eudendrium* sp.) (2.3%). Along the transect, 7 fish species were observed: *S. salpa* (5.9 %), followed by *D. vulgaris* (4.7%) and *O. melanura* (3.5%). Lower frequencies were recorded for *C. chromis*, *C. julis* (both 2.4%), *T. pavo* and *M. barbatus* (both 1.2%).

At transect 4 (approx. 4-4.5 m depth; 89 plots examined), the bottom is mainly characterized by sand (83.1%) covered by *P. oceanica* (77.5%). Lower frequencies were recorded for stones (43.8%) and boulders/rock (7.9%), which show high mean coverage percentages, 88.3% for boulders/rocks and 92.5% for stones. Only low intensity gas emissions were observed in 2 scattered and 4 continuous plots. The species showing the high frequencies were *P. pavonica* (33.7%), *J. rubens* (13.5%) and *S. foetidus* (7.9%). Lower frequencies were recorder for the sponge *C. crambe* (1.1%) and the alga *A. stellata* (3.4 %). Six species of fish were encountered: *C. chromis* (21.3%), *S. maena* (7.9%), *O. melanura* (5.6%), *C. julis* and *D. vulgaris* (both with 2.2%), and *T. pavo* (1.1%).

Discussions and conclusions

The shallow CO_2-rich hydrothermal vents of volcanic origin offer unique opportunities to study the vulnerability of coastal ecosystems to ocean acidification [41]. In this paper, we described the vents of San Giorgio (Southern Tyrrhenian Sea), whose discovery is new for science. This area both for physico-chemical proprieties and for easy accessibility can be elected as a suitable natural laboratory for ocean acidification research, as well as on changes in structure of the benthic and fish assemblages and habitat complexity [42].

In our study area, the lower pH value recorded was 7.84, which is equivalent to what scientists have predicted by the year 2100 [43, 44]. This value is comparable to what occur at the Ischia-Castello Aragonese intermediate vents area [S2 and N2 stations in various papers,13]. However, at the Ischia vents the pH_T showed a wide variability [45, 41], and a clear gradient ranging from pH_T values < 6 to 8.1 is realized from high venting zones to outside the vent area.

The San Giorgio pH range, moreover, is similar to low pH zone of Baia di Levante in Vulcano (7.84 ± 0.24 pH) [46], and to the rim zone around the Bottaro crater off Panarea island [47], while off Panarea around the Basiluzzo islet, very low values were recorded (pH_T 4.7-5.4) [48]. The lower values of geochemical parameters were all recorded in the central part of our study area, that

correspond with the area in which the higher intensity of gas emissions was detected. Dissolved organic nutrients showed relatively low concentration, and the higher values recorded in the external part of the area of gas emissions could be of anthropogenic origins linked to the nearby bathing beach.

The gas emitted at the San Giorgio hydrothermal vents show a predominant CO_2 concentration, similar to those recorded at Levante Bay (Vulcano island) (97-99%) [46], and slightly higher than that at Castello Aragonese (90–95%) [13, 37]. The percentage of H_2S (0.35%) in San Giorgio is lower than at Vulcano (2.2%) [49], while at the Castello Aragonese no sulphur was recorded [13, 37]. This very low percentage of H_2S is very important to conduct studies on the response of species and community to ocean acidification. Indeed, the concurrent presence of CO_2 with other toxic gases makes difficult disentangle the negative effects of OA by those of the other dangerous substances [18, 19]. The high R/Ra values recorded in San Giorgio vents could be assumed to be related to the ascent of heat and deep-seated magmatic fluids to the surface. These values are similar to those measured at Capo Calavà (R/Ra = 2.5), in a gas sample collected about 2 km WNW of the investigated area by Sano et al. [50]. The value of $\delta^{13}C_{CO2}$ seems to confirm an inorganic origin of hydrothermal degassing of CO_2 [50]. Although no substantial temperature differences were recorded in our study, the sub-circular rusty patches observed could testify a rising of mineral-enriched columns of fluid into the seafloor. However, this aspect needs more appropriate investigations. In addition, considering that the San Giorgio vents are located in the vicinity of the Aeolian-Tindari-Letojanni faults system, it is not excluded that there may be additional yet unexplored emission zones. For this, other in-depth studies should be conducted in the nearby areas.

Most of the species recorded in San Giorgio vents are typical of shallow photophylous vegetated habitat and are commonly recorded in similar areas not subjected to gas emissions. The main algae dominating the rock and boulder coverage are typical of the summer season (e.g., *P. pavonica, H. scoparia*); new important information would be acquired sampling at the vents in different seasons. However, the dominating taxon, along the whole transects and depths examined, is the sponge *Sarcotragus foetidus*. Sponges are quite robust to OA, as proved by their occurrence at other vent's systems as at the Castello Aragonese [51], the Grotta del Mago cave [37], and the Vullatura vents at Ischia; although in this latter system the community is dominated by *Crambe crambe* settled on the dead matte of *Posidonia oceanica* [37].

The fish fauna resembles that found in other analogous areas in Mediterranean Sea, and has been reported also for the vents at the Castello in Ischia and at Levante Bay in Vulcano [52]. Some species found in our study as *S. salpa, C. chromis, C. julis* are known for their tolerance to acidification [52]. Although experimental studies have shown some negative effects of acidification on fish physiology and behaviour, especially on the juvenile stages [52, 53], we found juveniles of several species. In San Giorgio, we recorded five species listed in Annexes I and II of the SPA/BIO Protocol of the Barcelona Convention: the scleractinian *Cladocora caespitosa*, the sponge *Sarcotragus foetidus*, the sea urchin *Paracentrotus lividus*, the bivalve *Pinna rudis* and the seagrass *Posidonia oceanica*. In addition, juveniles of *Epinephelus costae* and *E. marginatus*, considered respectively as vulnerable and endangered species in the red list of threatened species enacted by the International Union for Conservation of Nature (IUCN), were also recorded. Finally, alien species recorded at San Giorgio are limited to the alga *C. cylindracea* and the decapod *P. gibbesi*, while in other vents systems alien organisms are often quite common since favoured by low competition [29].

In conclusion, this study describes the hydrothermal vents system of San Giorgio, in Gioiosa Marea, characterized by prevalent CO_2 emissions and negligible occurrence of other potential toxic compounds such as H_2S. For these reasons, we believe that it could be elected as a suitable natural laboratory to study the OA effects on process in marine ecosystems, especially using an experimental approach due to its easy accessibility and shallow depths.

Despite hydrothermal vents are recognized hot spot of biodiversity and supply high services to humans, in the Mediterranean Sea they are not subjected to any protection. In Natura 2000 Network [54] the habitat #1180, defined as "Submarine structures made by leaking gases", is considered a habitat to protect, however, this definition is vague and seems more oriented to the geological setting of the bottom, than to its biological features. We think that for the rarity and the ecological and evolutionary relevance of these environments, the definition of the habitat 1180 should be better explicated to include also the biotic components associated to hydrothermal vent systems, and their large variability at local scale. Shallow vents should be more protected by conservation measures and greater attention should be given by Authorities to these unique systems.

Material and Methods

Sampling survey

An explorative survey, conducted in May 2021 and aimed to drawing up the sampling plan, and select the most appropriate survey technique, showed that the emissions were scattered in a rectangular area about 200 m long, and up to 40 m from the coastline. Within this area, two parallel survey designs were planned to characterize the chemical features and perform the visual census of the benthic and nektonic species, respectively.

All samplings were carried out in June 2021. For the chemical analyses, five transects perpendicular to the coastline were considered (Figure 1, Supplement Table S1). A central transect (TR1) was established to intercept the point of highest bottom flow of emissions (SG2). Moving eastwards, the TR2 transect was in correspondence with the last emissions visible, and the TR3, about 100 m far from them. The remaining two transects were identified by moving westwards of TR1, respectively in correspondence with the last emissions visible (TR4) and about 100 m far from them (TR5). In each transect four sampling stations (SG) were located at 1, 20, 40 and 80 m away from the shoreline, reaching 4 m of maximum depth, for a total of 20 stations sampled. Water chemistry was analysed also in the points outside the gas emission area (transects TR3, TR5 and all sampling sites at 80 m from the coastline) to evaluate the influence of the emissions on the surrounding environment.

Biotic investigation was conducted by means of the underwater visual census (UVC) only in the area directly affected by the emissions (circumscribed by the red rectangle in Figure 1), through transects parallel to the coastline, which allow better appreciation of the local biodiversity along a similar depth. The UVC observation were conducted in four transects along the coastal length of the area (200 m) and distanced 10 m from each other, covering an area of about 8.000 m^2, and within a depth range from 1 to 4-5 m (Supplement 2).

Abiotic investigation

Water chemistry analyses

Water samples for salinity, pH, AT, dissolved inorganic nutrients and H_2S were collected by means of Niskin bottles along the five transects perpendicular to the coastline (TR1-TR5). For pH and AT

samples, 120 mL borosilicate glass bottles were filled with seawater and poisoned with 100 μL of saturated mercuric chloride ($HgCl_2$), and then stored at 4 °C in the dark, until analysis.

Dissolved inorganic nutrients samples were initially filtered by Whatman GF/F filters to remove phytoplankton cells and particles of $CaCO_3$, and then stored in 125 mL polyethylene jars. H_2S samples were collected in 40 mL vials adding 0.8mL zinc acetate (ZnC□H□O□) and then stored at 4 °C in the dark. Salinity was collected in 200 mL glass bottles and then stored at 4 °C in the dark. pH and AT analytic determinations were performed by means of spectrophotometer Cary 100 Scan UV-visible and Mettler Toledo G20 equipped with LAUDA L100, respectively, according to laboratory procedures described by Dickson et al. [55] and Urbini et al. [56].

Analyses were performed by the National Institute of Oceanography and Applied Geophysics (OGS) both at the laboratories located in Trieste and at the ECCSEL-ERIC NatLab Italy of Panarea.

Dissolved inorganic nutrients

The nitrite, nitrate, ammonium, phosphate and sulphate samples were prefiltered on 0.7 μm pore size glass-fibre filters (Whatman GF/F) immediately after the sampling and stored at −20 °C in polyethylene vials until analysis. The samples were defrosted and analysed colorimetrically with a Bran + Luebbe Autoanalyzer 3, according to Grasshoff et al. [57]. Detection limits for the procedure were 0.003 μM, 0.01 μM, 0.04 μM, 0.02 μM, and 0.02 μM for NO_2, NO_3, NH_4, PO_4, and H_4SiO_4, respectively.

Gas analyses

Gases have been sampled from submarine vents using an inverted funnel connected to two-way glass bottles [58]. The chemical and isotopic analysis were performed at laboratories of INGV-Palermo. The chemical composition of the bubbling gases was determined by gas chromatography (GC) using an Agilent equipped with a double TCD-FID detector and argon as carrier gas. The gaseous samples had been admitted to the GC by a syringe, and the uncertainties are within ±5%. Measurements of carbon isotopic compositions ($\delta^{13}C_{CO2}$) of the vented gases were made by a Delta Plus XP IRMS equipped with a Thermo TRACE GC interfaced with Thermo GC/C III. The results (expressed in $\delta^{13}C‰$) are relative to the V-PDB (Vienna-Pee Dee Belemnite) standard, and the standard deviation of the 13C/12C ratio was ±0.2‰. The He isotope ratio (3He/4He) was analysed by a Helix SFT-Thermo static vacuum mass spectrometer after purification of He under high vacuum and cryogenic separation from Ne. Helium isotope compositions are given as R/RA, namely, 3He/4He of the sample versus the atmospheric 3He/4He (RA = 1:386 × 10–6). Typical uncertainties are within ±5%.

To estimate the total gas output flux from sediments, five point-measurements of gas flux were performed calculating the emptying-time of a 1 L bottle connected to the bubbling point by an overturned funnel (Figure 4).

Figure 4: Measures of gas output flux from sediments by a INGV researcher at the San Giorgio vents.

These measures were recorded in areas characterized by low, medium and high fluxes, defined by a visual scuba inspection of the bubbling emissions.

Gas output concentration

These measures have been recorded by means of an innovative instrument made *ad hoc* for determining air-water gas exchange rates. It comprises a floating platform equipped with a specifically designed infrared (IR) spectrophotometer connected directly with the chamber. The main components are an infrared gas analyser (IRGA - CO_2 Infrared Gas Sensor Gascard NG 10%), a pump and accumulation chamber (Supplement 3).

Biotic investigation

Data on bottom features and associated benthic and nektonic organisms were acquired by high-definition cameras (Crosstour Action Cam 4K) videos and photos. The species directly identified in the field were reported on a slate (Supplement 2).

To calculate frequency, the videos of each transect parallel to the coast, at different distances and depths, were analysed by selecting a frame every 10 seconds, and corresponding to a bottom linear distance of 2-3 m. In the selected plots (approx. 1x1 m frame), we estimated the percentage cover of different substrate types, such as soft sediments (sands), stones (lower than 1 m size), boulders (< 1 m size) and rocks, and the seagrass *Posidonia oceanica*; we also annotated in each plot the benthic organisms (plant and animals) and fishes occurring. The frequency of these organisms in the whole transect was measured as percentage of their occurrence over the total plots examined (Supplement 2). The scientific name of each species identified was up-dated according to the WoRMS database (https://www.marinespecies.org/).

References

1. Yang, K. & Scott, S.D. Possible contribution of a metal-rich magmatic fluid to a sea-floor hydrothermal system. *Nature.* **383(6599),** 420-423(1996).

2. Sander, S.G., & Koschinsky, A. Metal flux from hydrothermal vents increased by organic complexation. *Nat. Geo.* **4(3),** 145-150 (2011).

3. Levin, L.A. *et al.* Hydrothermal vents and methane seeps: rethinking the sphere of influence. *Front. Mar. Sci*. **3,** 72 (2016)
4. McCollom, T. M. & Shock, E. L. Geochemical constraints on chemo-lithoautotrophic metabolism by microorganisms in seafloor hydrothermal systems. *Geochim. Cosmochim. Acta* **61(20),** 4375-4391 (1997).
5. Gurunathan, R., Rathinam, A. J., Hwang, J. S. & Dahms, H. U. Shallow Hydrothermal Vent Bacteria and Their Secondary Metabolites with a Particular Focus on Bacillus. *Mar. Drugs* **19(12),** 681 (2021).
6. Boetius, A. & Wenzhöfer, F. Seafloor oxygen consumption fuelled by methane from cold seeps. *Nat. Geosci.* **6(9),** 725-734 (2013).
7. Di Bella *et al*. Rolling Ironstones from Earth and Mars: Terrestrial Hydrothermal Ooids as a Potential Analogue of Martian Spherules. *Minerals* **11(5),** 460 (2021).
8. Martin, W., Baross, J., Kelley, D. & Russell, M. J. Hydrothermal vents and the origin of life. *Nat. Rev. Microbiol.* **6(11),** 805-814 (2008).
9. Tarasov, V.G., Gebruk, A.V., Mironov, A.N. & Moskalev, L.I. Deep-sea and shallow-water hydrothermal vent communities: two different phenomena? *Chem. Geol.* **224 (1-3),** 5-39 (2005).
10. Tarasov, V.G. Effects of shallow□water hydrothermal venting on biological communities of coastal marine ecosystems of the Western Pacific. *Adv. Mar. Biol.* **50,** 267-421 (2006)
11. Giangrande A., Gambi M.C., Micheli F. & Kroeker K.J. Fabriciidae (Annelida, Sabellida) from a naturally acidified coastal system (Italy) with description of two new species. *J. Mar. Biolog. Assoc.* **94(7),** 1417-1427 (2014).
12. Giangrande, A., Putignano, M., Licciano, M. & Gambi, M.C. The Pandora's box: Morphological diversity within the genus emAmphiglena/em Claparède, 1864 (Sabellidae, Annelida) in the Mediterranean Sea, with description of nine new species. *Zootaxa*, **4949(2),** (2021).
13. Foo, S.A., Byrne, M., Ricevuto, E. & Gambi, M.C. The carbon dioxide vents of Ischia, Italy, a natural laboratory to assess impacts of ocean acidification on marine ecosystems: an overview of research and comparisons with other vent systems. *Oceanogr. Mar. Biol. Ann. Rev.*, **56,** 237-310 (2018).
14. Dahms, H.U., Schizas, N.V., James, R.A., Wang, L. & Hwang, J.S.. Marine hydrothermal vents as templates for global change scenarios. *Hydrobiologia*, **818(1),** 1-10 (2018).
15. Gonzalez Delgado, S. & Hernadez, J.C. The importance of natural acidified systems in the study of ocean acidification: what have we learned? *Adv. Mar. Biol.***80,** 57-99 (2018).
16. Gonzalez Delgado, S. *et al.* Chemical characterization of Punta de Fuencaliente CO_2 seeps system (La Palma Island, NE Atlantic Ocean): a new natural laboratory for ocean acidification studies. *Biogeosciences* (2020).
17. Harvey, B.P., Kon, K., Agostini, S., Wada, S. & Hall□Spencer, J.M. Ocean acidification locks algal communities in a species□poor early successional stage. *Glob. Change Biol.* **27(10),** 2174-2187 (2021).
18. Foo, S.A. & Byrne, M. Forecasting impacts of ocean acidification on marine communities: Utilizing volcanic CO_2 vents as natural laboratories. *Glob. Change Biol.*, **27(10),** 1995-1997 (2021).
19. Zitoun, R. *et al.* A unique temperate rocky coastal hydrothermal vent system (Whakaari–White Island, Bay of Plenty, New Zealand): constraints for ocean acidification studies. *Mar. Freshw. Res.* **71(3),** 321-344 (2019).

20. Teixido Ullod N. *et al.* Functional biodiversity loss along natural CO_2 gradients. *Nat. Comm.* **9(1),** 10.1038/s41467-018-07592-1 (2018).
21. Gamo, T. & Glasby, G. P.. Submarine hydrothermal activity in coastal zones. In *Land and Marine Hydrogeology* . 151-163 (Elsevier 2003).
22. Gamo, T. *et al.* Acidic and sulfate-rich hydrothermal fluids from the Manus back-arc basin, Papua New Guinea. *Geology*, **25(2),** 139-142 (1997).
23. González-Vega, A. *et al.* Significant release of dissolved inorganic nutrients from the shallow submarine volcano Tagoro (Canary Islands) based on seven-year monitoring. *Front. Mar. Sci*, **6,** 829 (2020).
24. Rastrick, S. S. *et al.* Using natural analogues to investigate the effects of climate change and ocean acidification on Northern ecosystems. *ICES Journal of Marine Science*, **75(7)**, 2299–2311 (2018).
25. Zhang, Z. *et al.* Developments of Exploration and Detection of Shallow-Water Hydrothermal Systems. *Sustainability*, **12(21),** 9109 (2020).
26. Maggioni F. *et al.* The Bouraké semi-enclosed lagoon (New Caledonia) – a natural laboratory to study the lifelong adaptation of a coral reef ecosystem to extreme environmental conditions. *Biogeosciences*, **18,** 1–24 (2021).
27. Daskalopoulou K., D'Alessandro W., Longo M., Pecoraino G. & Calabrese S. Shallow Sea Gas Manifestations in the Aegean Sea (Greece) as Natural Analog to Study Ocean Acidification: First Catalog and Geochemical Characterization. *Front. Mar. Sci.* **8,** 775247; 10.3389/fmars.2021.77524 (2022).
28. Dando, P.R., Stüben, D. & Varnavas, S.P. Hydrothermalism in the Mediterranean sea. *Progress in Oceanography*, **44(1-3),** 333-367 (1999).
29. Hall-Spencer J.M. & Allen R. The impact of CO_2 emissions on "nuisance" marine species. *Res. Reports Biodiv Studies*, **4,** 33-46 (2015).
30. Italiano, F., Bonfanti, P. & Maugeri, S. R. Evidence of tectonic control on the geochemical features of the volatiles vented along the Nebrodi-Peloritani Mts (Southern Apennine Chain, Italy). *Geofluids*, 2019
31. Linares C. *et al.* Persistent natural acidification drives major distribution shifts in marine benthic ecosystems. Proceeding Royal Society B; 10.1098/rspb.2015.0587 (2015).
32. Dando, P. R. *et al.* Hydrothermal studies in the Aegean Sea. *Physics and Chemistry of the Earth, Part B: Hydrology, Oceans and Atmosphere*, **25(1),** 1-8 (2000).
33. Crisa, A., Lanza, S. & Randazzo, G. The Historical Evolution of the Tindari-Marinello Spit (Patti, Messina, Italy). In *Sand and Gravel Spits* 103-121 (Springer, Cham) (2015).
34. Cultrera F. *et al.* Structural architecture and active deformation pattern in the northern sector of the Aeolian-Tindari-Letojanni fault system (SE Tyrrhenian Sea-NE Sicily) from integrated analysis of field, marine geophysical, seismological and geodetic data. *Ital. J. Geosci.*, **136 (3),** (2017).
35. Cultrera F. *et al.* Active faulting and continental slope instability in the Gulf of Patti (Tyrrhenian side of NE Sicily, Italy): a field, marine and seismological joint analysis. *Nat.l Haz.***86,** 5253-9272; 10.1007/s11069-016-2547-y (2017).
36. Barberi F., Gasparini P., Innocenti F. & Villari L. Volcanism of the southern Tyrrhenian Sea and its geodynamics implications. *J. Geophys. Res.* **78(23),** 5221-5232 (1973).

37. Dewey J.F., Helman M.L., Turco E., Hutton D.H.W. & Knott S.D. Kinematics of the Western Mediterranean. Dietrich D. & Park R.G., *Geol. Soc. Spec. Publ.,* 45, (Ed. Alpine tectonics) 265–283 (Coward M.P 1989).

38. Faccenna C., Becker T.W., Lucente F.P., Jolivet L. & Rossetti F. History of subduction and back-arc extension in the central Mediterranean. *Geophys. J. Int.,* 145, 809–820; 10.1046/j.0956-540x.2001.01435 (2001).

39**.** Romano, D. *et al.* Hazard scenarios related to submarine volcanic-hydrothermal activity and advanced monitoring strategies: A study case from the panarea volcanic group (Aeolian islands, Italy). Special Issue Emerging Techniques for Monitoring Geofluids and Geothermal Activities, *Geofluids* 2019.

40. Esposito A., Giordano G. & Anzidei M. The 2002-2003 submarine gas eruption at Panarea volcano (Aeolian Islands, Italy): Volcanology of the seafloor and implications for the hazard scenario. *Mar. Geol.,* **227(1-2),** 119-134 (2006).

41. Kroeker, K.J., Micheli, F., Gambi, M.C. & Martz, T.R. Divergent ecosystem responses within a benthic marine community to ocean acidification. *Proc. Natl. Acad. Sci.*, **108 (35),** 14515-14520 (2011).

42. Fabricius, K.E., Kluibenschedl, A., Harrington, L., Noonan, S. & De'ath, G. (2015). In situ changes of tropical crustose coralline algae along carbon dioxide gradients. *Sci. Rep.*, **5(1),** 1-7.

43. Caldeira, K. & Wickett, M.E. Ocean model predictions of chemistry changes from carbon dioxide emissions to the atmosphere and ocean. *J. Geophys. Res. Oceans*, **110(C9),** (2005).

44. Figuerola, B. *et al.* A review and meta-analysis of potential impacts of ocean acidification on marine calcifiers from the Southern Ocean. *Front. Mar. Sci*. **8,** 24 (2021).

45. Hofmann G.E. *et al.* High-Frequency Dynamics of Ocean pH: A Multi-Ecosystem Comparison. PLoS One **6(12),** e28983; 10.1371/journal.pone.0028983 (2011).

46. Boatta, F. *et al.* Geochemical survey of Levante Bay, Vulcano Island (Italy), a natural laboratory for the study of ocean acidification. *Mar. Poll. Bull.* **73(2),** 485-494 (2013).

47. Esposito, V. *et al.* Structural and functional analyses of motile fauna associated to *Cystoseira brachycarpa* along a gradient of ocean acidification in a CO_2 vent system off Panarea island (Aerolian Islands, Italy). *J. Mar. Sci. Eng.* **10,** 451. 10.3390/jmse10040451 (2022).

48. Gugliandolo, C., Italiano, F. & Maugeri, T. The submarine hydrothermal system of Panarea (Southern Italy): biogeochemical processes at the thermal fluids-sea bottom interface. *Ann. Geophys.*, **49,** 2-3 (2006).

49. Mirasole, A. *et al.* S. Fish assemblages cope with ocean acidification in a shallow volcanic CO2 vent benefiting from an adjacent recovery area. *Mar. Environ. Res,* **157,**104851 (2020).

50. Sano, Y., Wakita, H., Italiano, F. & Nuccio, M. P. Helium isotopes and tectonics in southern Italy. *Geophys. Res. Lett.* **16(6),** 511-514 (1989).

51. Goodwin, C., Rodolfo-Metalpa, R., Picton, B. & Hall-Spencer, J.M. Effects of ocean acidification on sponge communities. *Mar. Ecol.* **35,** 41 - 49 (2013).

52. Mirasole, A., Badalamenti, F., Di Franco, A., Gambi, M. C. & Teixidó, N. Boosted fish abundance associated with Posidonia oceanica meadows in temperate shallow CO_2 vents. *Sci. Total Envir.* **771,** 145438 (2021).

53. Franke, A., Clemmesen, C. (2011). Effect of ocean acidification on early life stages of Atlantic herring (*Clupea harengus* L.). *Biogeosciences*, **8(12),** 3697-3707.

54. European Commission. (2007). Guidelines for the establishment of the Natura 2000 network in the marine environment. *Application of the Habitats and Birds Directives.*
55. Dickson, A.G., Sabine, C.L., & Christian, J.R. *Guide to Best Practices for Ocean CO_2 Measurements*, Vol. 3. Sidney. Canada: PICES Special Publication (2007).
56.Urbini, L., Ingrosso, G., Djakovac, T., Piacentino, S. & Giani, M. Temporal and spatial variability of the CO_2 system in a riverine influenced area of the Mediterranean Sea, the northern Adriatic. *Front. Mar. Sci*, **7,** 679 (2020).
57. Grasshoff, K., Kremling, K. & Ehrhardt, M. (1999). *Methods of Seawater Analysis*. Chapter 4: determination of nutrients. 159–228 (1999).
58. Italiano, F., Sasmaz, A., Yuce, G. & Okan, O.O. Thermal fluids along the East Anatolian Fault Zone (EAFZ): Geochemical features and relationships with the tectonic setting. *Chem. Geol*, **339,** 103-114 (2013).

Acknowledgements
The authors wish to thank Aqua Element Diving (San Giorgio) for their technical assistance in sampling activities, the IPANEMA HR project and the ECCSEL-ERIC - NatLab Italy managed by the OGS at Panarea, for logistic support.

Author contributions
M.D. conceptualization of the idea, sampling activities, article-writing, taxonomic determinations; M.C.G. conceptualization of the idea, sampling design, article-writing, taxonomic determinations; C. C. sampling activities, gas/ chromatography analyses; M.D.B. sampling activities and article-writing, V. E. sampling activities, pH analyses, A.G. sampling design, gas output analyses, article-writing; S. G. sampling activities, article-writing, taxonomic determinations; M.K. dissolved inorganic nutrients analyses, F.I. sampling activities, conceptualization, article-writing; G.L. sampling activities, gas flux analyses, G.S. sampling activities, L.U. sampling design, alkalinity analyses, biogeochemical parameters calculations; C.D.V. founding, conceptualization, sampling design, writing.

Data availability
All data are included in text, tables and supplementary files.

Competing Interests Statement
The authors declare no competing interests.

Funding
This study has been partially funding by ECCSEL NatLab- Italy project, funded by the Italian Ministry of University and Research (MUR) for the Italian participation at ECCSEL ERIC (European Carbon Dioxe Capture and Storage Laboratory Infrastructure).

Legend
Figure 1. The study site and sampling spots. The hydrothermal field of San Giorgio is highlighted by the red polygon. Map made by means of ArcMap 10.5, ESRI software.
Figure 2. Image of one of the high intensity gas emissions form the bottoms of the San Giorgio hydrothermal vents.
Figure 3. Natural Neighbour spatial interpolations of the main representative abiotic parameters recorded in the San Giorgio vents study area. Map made by means of ArcMap 10.5, ESRI software.

Figure 4. Measures of gas output flux from sediments by a INGV researcher at the San Giorgio vents.

Table 1. Chemical and isotopic compositions of the sampled gas emissions. All the chemical concentrations are expressed in mol%. The helium isotopic composition is expressed as R/Ra, where R is the 3He/4He ratio in the sample and Ra is the same ratio in the atmosphere. The carbon isotopic composition is given versus PDB.

Table 2. Percentage of CO_2 recorded on four samples of air-water layer collected on the SG2 station. Coordinate are expressed in UTM WGS84, 33 S Zone.

Table 3. Total output of gases and typologies of emission flux recorded on five different sites.